3D inversion of gravity and gravity gradiometry data using multinary transformation of the model parameters

Wei Lin[1], and Michael S. Zhdanov[1,2]*
[1]University of Utah; [2]TechnoImaging

Summary

In this paper we demonstrate that the multinary model transformation applied to the 3D gravity and gravity gradiometry inversion helps to recover the sharp contrasts of the density between the host media and anomalous targets. This concept is a generalization of the binary approach to the multinary density inversion, which uses given values of density and error functions to transform the density distribution into the desired step-function distribution. We solve the multinary inverse problem using the regularized conjugate gradient method. The novel gravity multinary inversion algorithm is demonstrated to be effective in determining the shape, location, and the densities of the anomalous targets. We also show that this method can be effectively applied to the inversion of the full tensor gravity gradiometry data computer-simulated for the SEG salt density model.

Introduction

Traditional methods of gravity inversion characterize the density distribution in the area of interest by a function, which varies continuously within the bounds. In order to ensure the unique and stable solution of the gravity inverse problem, one can impose additional conditions on the density, such as minimum norm (Tikhonov and Arsenin, 1977), or maximum smoothness (Constable, et al, 1987) or the fuzzy c-mean clustering method (Li and Sun, 2014). However, the inverse models produced by traditional inversions are still represented by a continuous distribution of the density over the anomalous targets. At the same time, typical geological structures, such as ore deposits, are usually characterized by a sharp boundary separating the target and a host rock.

In recent years, several techniques have been developed to recover anomalous targets with high contrasts between physical properties and sharp boundaries. For example, one can use focusing regularization (Portniaguine and Zhdanov, 1999; Zhdanov, 2002, 2009) to recover model parameters with sharp physical property contrasts; or the parametric level-set approach can be employed to represent the target based on octree-mesh inversion (McMillan et al., 2015). However, all these methods still produce a continuous distribution of the physical properties, even if the inverse images become more focused and sharp.

In this paper, we investigate a novel approach to inversion of the gravity data based on multinary transformation of the model parameters. This concept is a generalization of binary density inversion, which uses given values of density and error function to transform the density distribution into the desired step-function distribution (Zhdanov and Cox, 2013). Compared with some existing realizations of binary inversion, which are solved using stochastic optimization methods (e.g. Bosch et al., 2001; Krahenbuhl and Li, 2006), our approach is based on deterministic optimization methods, which can be applied to both linear and nonlinear inverse problems (Zhdanov, 2002, 2015).

Inverse problem formulation

The gravity inverse problem can be formulated as a solution of the following operator equation:

$$\mathbf{d} = \mathbf{A}(\boldsymbol{\rho}), \tag{1}$$

where **A** is a linear operator for computing the gravity field, d are the observed gravity field data, which may include the gravity field, G_z, and all components of the full gravity gradient tensor, and **ρ** represents the model density. In the case of a discrete inverse problem, the density distribution **ρ** can be represented as a vector formed by N_m components:

$$\boldsymbol{\rho} = [\rho_1, \rho_2, \dots, \rho_{N_m}]^T, \tag{2}$$

and the observed data d can be considered as an N_{d}-dimensional vector,

$$\mathbf{d} = [d_1, d_2, \dots, d_{N_d}]^T, \tag{3}$$

where the superscript *T* denotes the transposition operation. Usually, the inverse problem (1) is ill-posed, and we solve this problem using the regularization method by minimizing the corresponding parametric functional:

$$P^{\alpha}(\boldsymbol{\rho}) = ||\mathbf{W}_d(\mathbf{A}(\boldsymbol{\rho}) - \mathbf{d})||^2 + \alpha||\mathbf{W}_m(\boldsymbol{\rho} - \boldsymbol{\rho}_{apr})||^2 = min, \tag{4}$$

where $\mathbf{W}_d$ and $\mathbf{W}_m$ are the data and model weights, $\boldsymbol{\rho}_{apr}$ is the a-priori given density distribution, and α is a regularization parameter. This minimization problem (4) can be solved using the regularized conjugate gradient method (Zhdanov, 2002, 2015).

In a general case, the recovered density distribution is described by a continuous function. In some geophysical application, the desired physical property (e.g., density in the case of a gravity inverse problem) can be described by the binary function as follows:

$$\bar{m}_i = \left\{m_i^{(1)} = 0, m_i^{(2)} = 1\right\}, \tag{5}$$

or by the ternary function:

$$\bar{m}_i = \left\{m_i^{(1)} = -1, m_i^{(2)} = 0, m_i^{(3)} = 1\right\}. \tag{6}$$

Further, we can extend the description of the distribution of a physical property (e.g., density) using the multinary function of order *P*, having discrete numbers of values:

$$\bar{m}_i = \left\{m_i^{(1)}, m_i^{(2)}, \dots, m_i^{(P)}\right\}. \quad (7)$$

However, using such a multinary function in a regularized gradient type inversion makes it difficult to implement the derivative-based minimization of the Tikhonov parametric functional. Following Zhdanov and Cox (2013) and Zhdanov (2015), we can use a transformation of the model parameters and their sensitivities from their multinary-function representation to the representation of a continuous function. As a result, we will arrive at a conventional inverse problem and solve it using the regularized conjugate gradient method.

Multinary model transform

The nonlinear transformation of the multinary function into the continuous function, can be described as follows. We transform our density distribution, ρ_i, into a model space defined by a continuous range of multinary densities, $\tilde{\rho}_i$, using a superposition of error function:

$$\tilde{\rho}_i = E(\rho_i) = c\rho_i + \frac{1}{2}\sum_{j=1}^{P}\left[1 + \mathrm{erf}\left(\frac{\rho_i - \rho^{(j)}}{\sqrt{2}\sigma_j}\right)\right], \quad (8)$$

where $\boldsymbol{\rho} = \{\rho_i\}, i = 1, \dots, N_m$, is the original vector of the model parameters; $\tilde{\boldsymbol{\rho}} = \{\tilde{\rho}_i\}, i = 1, \dots, N_m$, is a new vector of the nonlinear parameters; and P is a total number of discrete (multinary) values of the model parameter (densities), $\rho^{(j)}$. The function $E(\rho_i)$ is the error function; parameter σ_j is a standard deviation of the value, $\rho^{(j)}$; and the constant c is a small number to avoid singularities in the calculation of the derivatives of the multinary densities.

All the desired densities, $\rho^{(j)}(j = 1, \dots, P)$, can be chosen a priori based on the known geological information (e.g., core samples). Note that, the derivative of the error function is equal to the corresponding Gaussian function, as follows:

$$\frac{\partial\tilde{\rho}_i}{\partial\rho_i} = g(\rho_i) = \frac{1}{\sqrt{2\pi}\sigma_j} e^{\frac{-\left(\rho_i - \rho^{(j)}\right)^2}{2\sigma_j^2}}. \quad (9)$$

Figure 1 represents an example of the error function and its derivative, Gaussian function, when $\tilde{\rho} = \{\rho_i^{(1)} = -1, \rho_i^{(2)} = 0, \rho_i^{(3)} = 1\}$ and $\sigma_j = 0.05(j = 1,2,3)$. Panel (a) shows that the approximate representation of the multinary model transform (8) can be interpreted as a cumulative density function of the densities, where the Gaussian function (9) means the probability density distribution of each discrete density ρ_i with the mean value $\rho^{(j)}$ and the standard deviation σ_j.

Inversion algorithm

As a result of the multinary model transform, the original density distribution, $\boldsymbol{\rho}$, has been changed into the transformed distribution, $\tilde{\boldsymbol{\rho}}$. Therefore, the original inverse problem (1) takes the following form:

$$\mathbf{d} = \tilde{\mathbf{A}}(\tilde{\boldsymbol{\rho}}), \quad (10)$$

where $\tilde{\mathbf{A}}$ is the new forward modeling operator acting in the transformed model space, $\tilde{\boldsymbol{\rho}}$. This nonlinear operator can be determined from equation (8) using the original linear operator $\mathbf{A}$ as follows:

$$\mathbf{d} = \tilde{\mathbf{A}}(\tilde{\boldsymbol{\rho}}) = \mathbf{A}[E^{-1}(\tilde{\boldsymbol{\rho}})]. \quad (11)$$

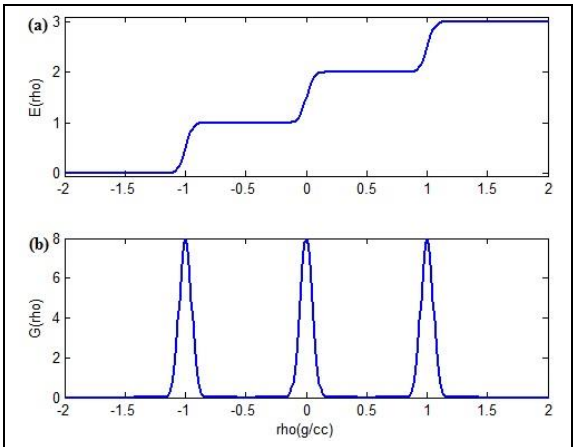

Figure 1: An example of the multinary function of the third order: (a) a combination of the error function, (b) its derivative, a combination of the Gaussian function. The values of the discrete densities are as follows: -1.0 g/cm^3, 0.0 g/cm^3, 1.0 g/cm^3, and $\sigma_j = 0.05(j = 1,2,3)$.

We solve this problem based on the minimization of the following Thikhonov parametric functional:

$$P^{\alpha}(\tilde{\boldsymbol{\rho}}) = ||\mathbf{W}_d(\tilde{\mathbf{A}}(\tilde{\boldsymbol{\rho}}) - \mathbf{d})||^2 + \alpha_n||\mathbf{W}_m(\tilde{\boldsymbol{\rho}} - \tilde{\boldsymbol{\rho}}_{apr})||^2 = min, \quad (12)$$

where $\mathbf{W}_d$ and $\mathbf{W}_m$ are data and model weights, respectively. We apply the regularized conjugate gradient (RCG) method (Zhdanov, 2002, 2015) for minimizing the parametric functional (12).

Synthetic model study

Synthetic model 1: Two-body model

In this section we test the developed algorithm of multinary inversion using a 3D synthetic model with two bodies with different sizes, densities and burial depths: the small and shallow one has the anomalous density of -1g/cm^3, where the density of the big and deep body is 0.5g/cm^3(see Figure 2, panel b). The value of the background density was set at 0. The synthetic gravity field, G_z, contaminated by 3% random noise, was used as the observed data. The multinary function was set to recover three discrete densities of 0g/cm^3, -1g/cm^3 and 0.5g/cm^3. The iterative inversion was run until the misfit reached the level of 3%.

Figure 2, panel (a), presents the profiles of the predicted gravity field (solid line) and the synthetic gravity field G_z (dotted line), obtained by the inversion, at Y=3750m (Northing). Panel (b) in the same Figure shows the vertical cross section of the synthetic model, corresponding to this profile, while panel (c) and (d) provide the same cross sections of the recovered density distribution using conventional inversion and multinary inversion, respectively. One can see that the conventional inversion failed to recover the correct values of the densities and locations of the anomalous bodies, however the multinary inversion successfully recovered the target bodies. Figure 3 presents a 3D view of the true Model 1 (panel a), and the multinary inversion result (panel b). Thus, the multinary inversion is able to image both the shallow and deep bodies at their true locations and densities.

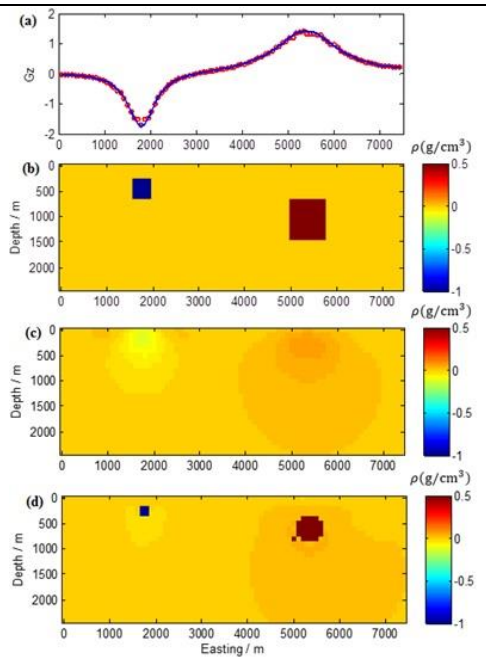

Figure 2: Model 1. Panel (a): Predicted gravity field (solid line) vs. synthetic gravity field G_z (dotted line) along the profile at Y=3750m (Northing). Panel (b): vertical cross section of the synthetic model. Panel (c) and (d) provide the same cross sections of the recovered density distribution using the conventional inversion and multinary inversion, respectively.

Synthetic model 2: Modified SEG salt dome model

In this section we will use the SEG salt dome model to test the multinary inversion. We have simplified the SEG salt model slightly by considering the anomalous targets associated with the salt dome only. Figure 4 shows a 2D cross section of the SEG salt model (modified after Boonyasiriwat, 2009), where the red part shows the salt body. The density of salt dome was set as -0.5g/cm^3 and the value of background density was 0.

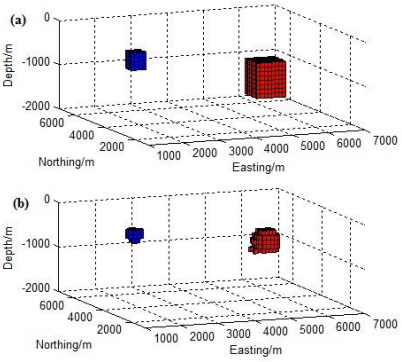

Figure 3: Model 1. 3D views of the synthetic model (panel a) and the inversion result (panel b).

The synthetic full tensor gravity gradiometry (FTG) data were used as the observed data and were contaminated by 3% random noise. In this synthetic model study the multinary inversion was set to recover two discrete densities of 0g/cm^3 and -0.5g/cm^3. We ran the iterative inversion until the final misfit value reached 3% at iteration number 170. Figure 5 shows a comparison between the synthetic data (dotted lines) used for multinary inversion and the predicted data (solid lines) for the FTG components, G_{zz}, G_{zx}, G_{zy}, G_{xx} and G_{yy}, at Y=2300m (Northing). One can see a very good data fitting. The vertical cross section of the synthetic model is given in Figure 5 (f), while panels (g) and (h) show the cross sections of the recovered models using the conventional smooth and multinary inversions, respectively. One can see that, the conventional inversion can only show a weak anomaly near the surface; however the multinary inversion recovers the approximate location and shape of the salt dome at its true density very well. Figure 6 presents a 3D view of the true Model 2 (panel a), and the multinary inversion result (panel b). Thus, the inversion results demonstrate that the multinary inversion approach has a strong potential to improve the quality of the gravity inversion for geological targets with sharp density contrast, e.g., a salt dome structure.

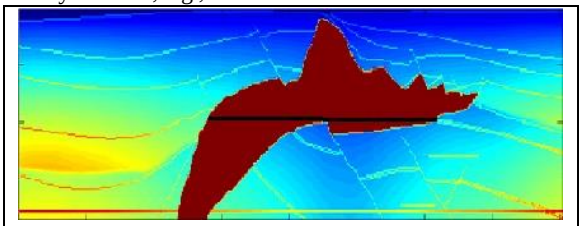

Figure 4: A 2D cross section of the SEG salt model (modified after Boonyasiriwat, 2009).

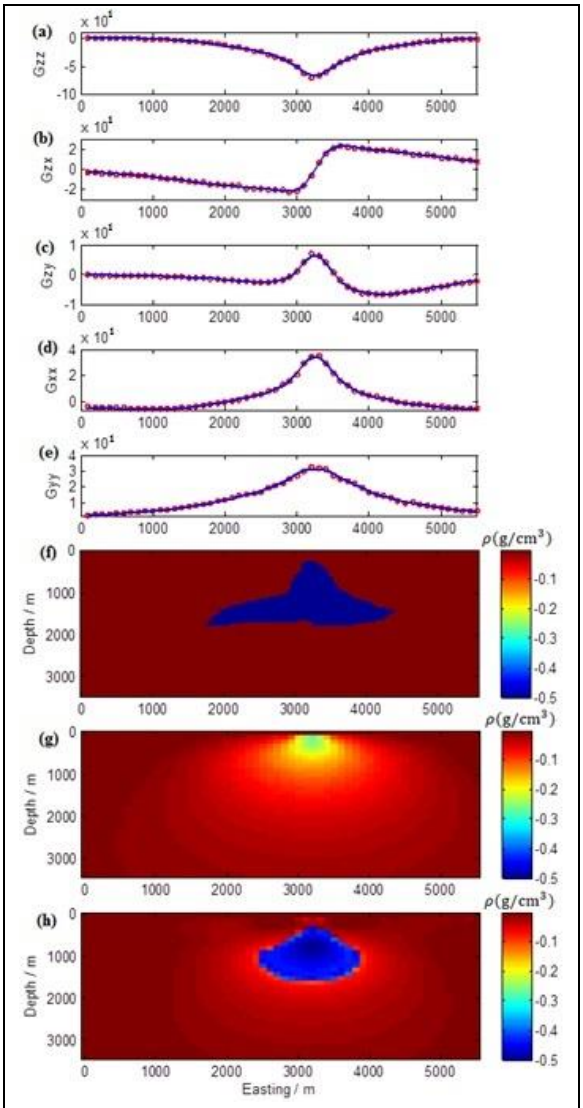

Figure 5: Model 2: Predicted gravity field (solid line) vs. synthetic FTG data (dotted line) along the profile at Y=2300m (Northing) for (a) G_{zz}, (b) G_{zx}, (c) G_{zy}, (d) G_{xx} and (e) G_{yy} components. Panel (f) presents the vertical cross section of the synthetic model. Panels (g) and (h) provide the same cross sections of the recovered density distribution using conventional inversion and multinary inversion, respectively.

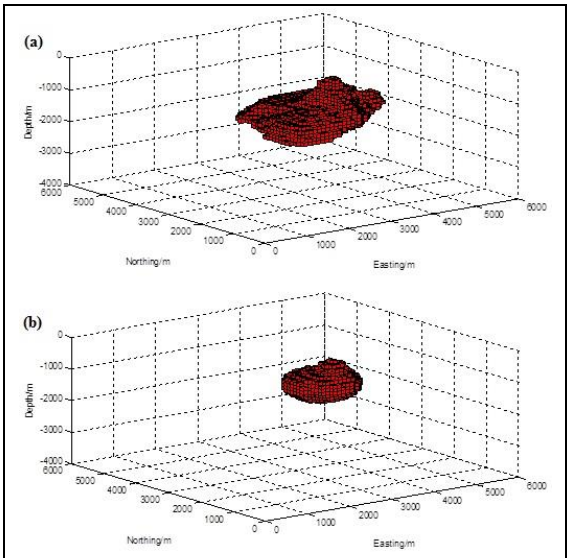

Figure 6: Model 2. 3D views of the synthetic model (panel a) and the inversion result (panel b).

Conclusion

We have applied a multinary inversion to solve the gravity and gravity gradiometry inverse problem with the anomalous bodies characterized by a finite number of discrete values of the densities. We have demonstrated that this inverse problem can be solved using deterministic optimization methods (Zhdanov, 2002). We have tested this method with two 3D synthetic models: a two-body model and a modified SEG salt dome density model. The results of our modeling studies demonstrated that multinary inversion can recover the approximate shapes and locations of the anomalous bodies and their densities well. Thus, the results of our study demonstrate that the novel multinary inversion approach has a strong potential to improve the quality of the gravity inversion for geological targets with sharp density contrast, e.g., a salt dome structure.

Acknowledgements

The authors acknowledge support from the University of Utah's Consortium for Electromagnetic Modeling and Inversion (CEMI), and TechnoImaging.

EDITED REFERENCES

Note: This reference list is a copyedited version of the reference list submitted by the author. Reference lists for the 2016 SEG Technical Program Expanded Abstracts have been copyedited so that references provided with the online metadata for each paper will achieve a high degree of linking to cited sources that appear on the Web.

REFERENCES

Boonyasiriwat, C., 2009, Acoustic waveform inversion of two-dimensional Gulf of Mexico data: M.S. thesis, The University of Utah.

Bosch, M., A. Guillen, and P. Ledru, 2001, Lithologic tomography: An application to geophysical data from the Cadomian belt of northern Brittany, France: Tectonophysics, **331**, 197–227, http://dx.doi.org/10.1016/S0040-1951(00)00243-2.

Constable, S. C., R. L. Parker, and C. G. Constable, 1987, Occam's inversion: A practical algorithm for generating smooth models from electromagnetic sounding data: Geophysics, **52**, 289–300, http://dx.doi.org/10.1190/1.1442303.

Krahenbuhl, R. A., and Y. Li, 2006, Inversion of gravity data using a binary formulation: Geophysical Journal International, **167**, 543–556, http://dx.doi.org/10.1111/j.1365-246X.2006.03179.x.

Li, Y., and J. Sun, 2014, Total magnetization vector inversion using guided fuzzy c-means clustering: 84th Annual International Meeting, SEG, Expanded Abstracts, 5183, http://dx.doi.org/10.1190/segam2014-1041.1.

McMillan, M. S., C. Schwarzbach, E. Haber, and D. Oldenburg, 2015, 3D parametric hybrid inversion of time-domain airborne electromagnetic data: Geophysics, **80**, no. 6, K25–K36, http://dx.doi.org/10.1190/geo2015-0141.1.

Portniaguine, O., and M. S. Zhdanov, 1999, Focusing geophysical inversion images: Geophysics, **64**, 874–887, http://dx.doi.org/10.1190/1.1444596.

Tikhonov, A. N., and V. Y. Arsenin, 1977, Solutions of ill-posed problems: V. H. Winston and Sons.

Zhdanov, M. S., 2002, Geophysical inverse theory and regularization problems: Elsevier.

Zhdanov, M. S., 2009, New advances in regularized inversion of gravity and electromagnetic data: Geophysical Prospecting, **57**, 463–478, http://dx.doi.org/10.1111/j.1365-2478.2008.00763.x.

Zhdanov, M. S., 2015, Inverse theory and applications in geophysics: Elsevier.

Zhdanov, M. S., and L. Cox, 2013, Multinary inversion for tunnel detection: IEEE Geoscience and Remote Sensing Letters, **10**, 1100–1103, http://dx.doi.org/10.1109/LGRS.2012.2230433.